Clim. Past Discuss., doi:10.5194/cp-2016-87, 2016
Manuscript under review for journal Clim. Past
Published: 29 August 2016

Climate of the Past Discussions
Open Access
EGU

Summer precipitation reconstructed quantitatively using a Mid Holocene $\delta^{13}C$ common millet record from Guanzhong Basin, China

Qing Yang[1, 2], Xiaoqiang Li[2]*, Xinying Zhou[2], Keliang Zhao[2] & Nan Sun[3]

1. School of Geography Science, Nanjing Normal University, Nanjing, 210023, China
2. Key Laboratory of Vertebrate Evolution and Human Origin of Chinese Academy of Sciences, Institute of Vertebrate Paleontology and Paleoanthropology, Chinese Academy of Sciences, Beijing, 100044, China
3. The School of Earth Science and Resources, Chang'an University, Xi'an, Sha'anxi, 710054, China

*Correspondence and requests for materials should be addressed to X.L. (lixiaoqiang@ivpp.ac.cn)

Abstract

In order to produce quantitative Holocene precipitation reconstructions for particular geographical areas, explicit proxies and accurate dating controls are required. The fossilized seeds of common millet (*Panicum miliaceum*) are found throughout the sedimentary strata of northern China, and are highly suited to the production of accurate quantitative Holocene precipitation reconstructions: their isotopic carbon composition ($\delta^{13}C$) gives a measure of the precipitation required during the growing season, and allows these seeds to be dated. We therefore used a robust regression function, as part of a systematic study of the $\delta^{13}C$ of common millet, to produce a quantitative reconstruction of Mid Holocene summer precipitation in the Guanzhong Basin. Our results showed that summer precipitation from 7.7-3.4 ka BP was 240-477 mm, with a mean of 354 mm, *i.e.* ~50 mm or 17% higher than present levels. Maximal mean summer precipitation peaked at 414 mm, ~109 mm (or 36%) higher than today, occurring during 6.4-5.5 ka BP; this is when the East Asian Summer Monsoon (EASM) was at its peak. As the $\delta^{13}C$-based precipitation record can reliably indicate EASM intensity during the Holocene, this work can provide a reliable proxy for further research into the detailed processes, and precise mechanisms, of the EASM.

Keywords: summer precipitation; quantitative reconstruction; Holocene; Chinese Loess Plateau; common millet; stable carbon isotope

Sect.

1 Introduction

The reconstruction of global climate changes through history is an important part of the Past Global Changes (PAGES) project. Such reconstructions provide an attempt to understand the evolution of the earth's climate over time, and any temporal, spatial and/or regional differences. Quantitatively reconstructing climatic factors such as temperature and precipitation provides an understanding of agricultural development and the human impact upon the landscape and environment. However, modern records are insufficient for the accurate documenting of the drivers of climate change, since they cover only the past century or so (De Menocal, 2001). The quantitative

Clim. Past Discuss., doi:10.5194/cp-2016-87, 2016
Manuscript under review for journal Clim. Past
Published: 29 August 2016

Climate of the Past Discussions
Open Access
EGU

reconstruction of temperature and precipitation using high resolution climatic proxy records has therefore become the principal thrust of PAGES research. To this end, we chose an area key to the warm period of the Holocene to produce a quantitative precipitation reconstruction for that geological time.

The Holocene, as the most recent geological period, has witnessed the emergence and rapid development of primitive farming, and therefore has the closest relation to human survival and development. The Holocene has experienced three distinct climatic phases: a rapid warming during the Early Holocene; a warm and humid Mid Holocene phase; and a gradual cooling during the Late Holocene (An *et al*., 2000; Wang *et al*., 2005a). The Holocene has also seen climatic fluctuations caused by rapid climate change and other catastrophic events such as flooding, drought and intense tropical cyclones (Bond *et al*., 1997; Mayewski *et al*., 2004; Kleiven *et al*., 2008). The megathermal phase of the Mid Holocene is similar to a scenario whereby global average temperatures rise by 1～2ºC (Prentice and Webb, 1998), and can therefore be regarded as a paleoanalog for future climate prediction and the evaluation of potential environmental impacts.

Centennial scale quantitative paleoclimatic reconstructions are needed if we are to understand more completely and accurately climate change processes and controls. To date, most continental paleoclimate studies have focused on temperature (Porter and An, 1995; Guo *et al*., 1996; Genty *et al*., 2003; Wang *et al*., 2008; Sun *et al*., 2012). Reconstructions of regional and global temperatures have shown that the warm Early Holocene (10-5 ka BP) was followed by a 0.7°C cooling through the Mid to Late Holocene (<5 ka BP), reaching a minimum ~200 years ago, during the 'Little Ice Age'. The recent rapid warming of the climate is unprecedented, based on surface temperature reconstructions for the past 1,500 years (Marcott *et al*., 2013). However, the increase in global surface temperatures has tended to cause changes in precipitation and atmospheric moisture through changes in atmospheric circulation, a more active hydrological cycle and an increasing water holding capacity throughout the atmosphere (Dore, 2005). The availability of water, one of the major challenges for the future, cannot be ignored, due to its significant role in the hydrological cycle (Hetté and Guiot, 2005).

The EASM, an important component of the Asian Summer Monsoon (ASM), plays an indispensable role in the hydrological cycle over southern China. Various proxies have been adopted in studies of the EASM during the Holocene. Due to their reliable chronology and relatively easy dating, oxygen isotopes ($\delta^{18}O$) in speleothems from Chinese caves have been taken as a robust measure of summer monsoon precipitation values (Wang *et al*., 2005a; Cheng *et al*., 2009). However, the interpretation of these changes in the $\delta^{18}O$ values of precipitation remains highly controversial; some scientists have contended that the stalagmite $\delta^{18}O$ record from the EASM region may not record EASM variability (Le Grande and Schmidt, 2009; Maher and Thompson, 2012; Tan, 2012; Caley *et al*., 2014; Liu *et al*., 2015).

The Chinese Loess Plateau (CLP), located in a transition zone between a semi-arid and semi-humid climate, and being deeply impacted by the EASM, is, and has been, highly sensitive to changes in precipitation and has thus long been a key area for

Clim. Past Discuss., doi:10.5194/cp-2016-87, 2016
Manuscript under review for journal Clim. Past
Published: 29 August 2016

Climate of the Past Discussions
Open Access
EGU

EASM research. The quantitative precipitation reconstruction results obtained have been based exclusively on climatic proxies derived from the CLP's geological and biological records. In the western CLP, fossil charcoal records in the Tianshui Basin have demonstrated that the mean annual precipitation (MAP) was 688-778 mm between 5.2-4.3 ka BP (Sun and Li, 2012). In the CLP's hinterland, magnetic susceptibility records from the Luochuan profile have provided estimates of Holocene MAP varying between 600 and 750 mm, with a mean value of 701±74 mm (Lu *et al*., 1994). In the southern CLP, Guanzhong Basin MAP, as revealed by plant phytolith assemblies, was 700–800 mm during the Holocene, indicating a much more humid climate than today's (Lu *et al*., 1996). Further evidence from the transfer functions of geological records and the intensity of pedogenesis has shown that Guanzhong Basin MAP was >700 mm during the Holocene Optimum (Sun *et al*., 1999; Zhao, 2003), supporting the aforementioned results. However, due to their intrinsic limitations, such as discontinuity and an indefinite response mechanism between the proxies and climate change, these tentative proxies have not been extensively applied. This has led to either short-term or/and unverifiable quantitative results. Selecting an effective proxy which evinces a continuous distribution, reliable dating and an unambiguous implication is crucial for the quantitative reconstruction of paleoprecipitation. High-resolution pollen-based quantitative precipitation results indicating EASM evolution have recently been obtained from an alpine lake in northern China (Chen *et al.*, 2015). However, because these are attributable solely to this unique environment, a regional quantitative precipitation reconstruction, and therefore a new proxy, is still required.

Common millet (*Panicum miliaceum*), as the most representative agricultural rain-fed crop of northern China, contains $\delta^{13}C$; this is sensitive to precipitation and can thus effectively record precipitation during the growing season (Yang and Li, 2015). Rain-fed agriculture originated in the CLP, giving rise to the first recognizably Chinese civilization. Many archeological relics from an unbroken historical continuum are therefore found throughout the region (An, 1988). Quantities of the fossilized seeds of common millet are well-preserved in the cultural layers of these archeological sites (Zhao and Xu, 2004; Liu *et al*., 2008; Lu *et al*., 2009). Their stable $\delta^{13}C$ compositions, which remain little change because of the low temperatures associated with carbonization, contain valuable information about paleoclimate change and early agricultural activities (Yang *et al*., 2011a, 2011b). Common millet remains are therefore perfect for quantitatively reconstructing Holocene precipitation in the CLP.

The Guanzhong Basin (Figure 1), in the southern CLP, was the cradle of Neolithic culture and China's ancient civilization, and fostered the Laoguantai (~7.8-6.9 ka BP), Yangshao (~6.9-5.0 ka BP) and Longshan (~5.0-4.0 ka BP) cultures (Ren and Wu, 2010), the pre-Zhou culture (~3.5-3.0 ka BP) (Lei, 2010), and the Zhou dynasties. Due to the intensity of early agricultural activity, huge quantities of common millet remains have been preserved in numerous, continuously-occupied cultural sites. Carbonized common millet seeds are the most abundant resource found in the samples collected in this study from these cultural layers.

In this study, common millet remains, from five sections characterized by

Clim. Past Discuss., doi:10.5194/cp-2016-87, 2016
Manuscript under review for journal Clim. Past
Published: 29 August 2016

Climate of the Past Discussions
Open Access
EGU

continuous and well-developed sedimentation at typical archeological sites, including the Baijiacun (BJC), Huiduipo (HDP), Manan (MN), Beiniu (BN) and Nansha (NS) sites (Figure 1), were sampled as part of a systematic study of $\delta^{13}C$ records; quantitative precipitation reconstructions for the Holocene were then based upon a robust transfer function between the $\delta^{13}C$ of modern common millet and precipitation, providing a scientific basis for predicting future climate change and its possible impact.

2 Methods

2.1 Sampling

All the ancient common millet remains used in this study were found at five archeological sites in the Guanzhong Basin, *i.e.* the BJC, HDP, MN, BN and NS sites (State Cultural Relics Bureau, 1998). Five sections characterized by continuous and well-developed sedimentation were selected for sampling at the BJC, BN, HDP, MN and NS sites. The sampling interval was 10 cm for the BJC and NS sections, and 20 cm for the BN, HDP and MN sections. Forty litre sample bags were filled with sufficient quantities of sedimentary material to screen through a 50-mesh sieve to obtain samples using flotation (Tsuyuzaki, 1994). Different archeological remains were separated in the laboratory after air-drying. Agricultural seeds were identified and picked out under the stereomicroscope, then marked in order according to sampling depth. The numbers of remnant common millet seeds derived from all five sections are listed in Table 1.

2.3 Stable $\delta^{13}C$ analysis

Stable $\delta^{13}C$ composition analyses were carried out on all 67 serial and bulk common millet samples from the five sections, each composed of three to five grains, without lemma. Each sample portion was placed in a beaker and covered with a 1% hydrochloric acid solution to remove any carbonates. The samples were then washed with distilled water to pH >5 and oven dried at 40°C for 24 h. The dried samples were ground in an agate mortar and homogenized, then vacuum-sealed in a quartz tube with copper oxide and silver foil and combusted for at least 4 h at 850°C. The CO_2 gas from the combustion tube was extracted and cryogenically purified. The isotopic ratio of the extracted CO_2 gas was determined using a MAT-251 gas source mass spectrometer with a dual inlet system at the Institute of Earth Environment, Chinese Academy of Sciences.

All isotope ratios were expressed using the following δ notation:

$$\delta^{13}C(‰) = [(R_{sample} - R_{std})/R_{std}] \times 1000 \qquad \text{Eq. (1)}$$

The isotopic standard used was Vienna Pee Dee Belemnite (VPDB); analytical precision at the 1r level was reported as 0.2‰.

2.3 ^{14}C dating and age model

AMS ^{14}C dating was conducted on one charcoal fragment and one charred seed of common millet from the BJC section, five charred seeds each from the HDP and BN sections, one charred seed from the MN section, and three charred seeds from the NS

Clim. Past Discuss., doi:10.5194/cp-2016-87, 2016
Manuscript under review for journal Clim. Past
Published: 29 August 2016

Climate of the Past Discussions
Open Access
EGU

section. AMS ^{14}C dating was carried out in the AMS chemistry laboratories at the Australian Nuclear Science and Technology Organisation (ANSTO) using a STAR Accelerator. AMS ^{14}C dates were calibrated using Calib Rev 7.0.4 software and the INTCAL13 dataset (Reimer *et al*., 2013). The AMS ^{14}C dating results (Table 2) show that the ages of the sampled sections' cultural layers were usually correspondent with archeological periodization.

On the basis that the depth-based linear interpolation method was not fit for the dating of cultural layers because of potential disturbance, all common millet remnant samples were divided into several groups to guarantee at least one dating dataset for each group, as follows: samples from adjacent depths with close $\delta^{13}C$ values were placed in the same group, allowing a greater difference between each group (One-factor Analysis of Variance (one-way ANOVA), $P<0.05$).

2.4 Quantitative modeling method and data analysis

The results for $\delta^{13}C$ values in the seeds of modern millet grown on the CLP (ref. Yang and Li, 2015), demonstrated that the $\delta^{13}C$ of common millet has a significant positive correlation with precipitation. In this study, standard major axis regression analysis (SMA) was applied to establish a regression model between the $\delta^{13}C$ of modern common millet and precipitation during growing seasons. SMA is appropriate for random samples because, in data statistics analysis, it can take account of standard deviations in the fit of both independent variables and dependent variables. Moreover, any implication drawn from the dataset is both intuitionistic and perspicuous, and therefore superior to ordinary least squares (OLS). Any gradient acquired by SMA can more scientifically reflect the scaled relation between two sets of observations; the regression coefficient of data samples can then be solved by optimizing statistical responses in accordance with logical optimization criteria. Statistical analyses were conducted using SMATR software (Version 2.0) (Falster *et al.*, 2006). Other statistical analyses used SPSS 15.0 for Windows and OriginPro 8.0 software. Unless otherwise stated, differences were considered statistically significant when $P<0.05$.

3 Results

Carbonized seed remains, sampled from Neolithic cultural layers, have $\delta^{13}C$ values ranging from -11.11‰ to -9.26‰ (Figure 2a), with a mean of -10.23±0.36‰ ($n=66$, SD=±1 σ), eliminating the anomaly value of -8.82‰ analyzed by Boxplot using SPSS statistical software (Figure 2b). The $\delta^{13}C$ composition of modern common millet from the central and western CLP measured in 2008 ranged from -13.93‰ to -12.46‰, with a mean of -13.15±0.50‰ ($n=15$, SD=±1σ) (Yang and Li, 2015). It can thus be seen that the $\delta^{13}C$ values of common millet remains are more positive than those of modern seeds by ~2.92‰.

The ^{13}C composition of plants results from a combination of carbon isotope fractionation and source carbon isotope composition. Therefore, $\delta^{13}C$ changes in the atmosphere, as a part of total CO_2, are an important factor impacting upon the $\delta^{13}C$ values in plants (Araus and Buxo, 1993). The $\delta^{13}C$ values of atmospheric CO_2 in the

Clim. Past Discuss., doi:10.5194/cp-2016-87, 2016
Manuscript under review for journal Clim. Past
Published: 29 August 2016

Climate of the Past Discussions
Open Access
EGU

Holocene, from 11 ka BP to the pre-industrial age, show only a slight change, usually ranging between -6.1‰ and -6.6‰, with a mean value of -6.4± 0.15‰ (Marino *et al*., 1992; Leuenberger *et al*., 1992), ～1.8‰ higher than the present-day atmospheric CO_2 $\delta^{13}C$ values of -8.2‰ (Farquhar *et al*., 1989; Keeling and Whorf, 1992; Cuntz, 2011). After correcting for the change in atmospheric CO_2 $\delta^{13}C$ (1.8‰), the seed $\delta^{13}C$ values for Holocene millet from the Guanzhong Basin are equivalent to modern plant values of -12.01‰, and are therefore ～1.12‰ less depleted in $\delta^{13}C$ than modern seeds (for the t test, t=21.39).

The regression function between $\delta^{13}C$ and precipitation for the common millet growing season was established using SMA as follows (Figure 3):

$$\delta^{13}C\ (‰) = 0.0077P_{gp} - 14.76,\ r^2 = 0.56,\ P < 0.001 \qquad \text{Eq.(2)}$$

The function's gradient indicated that the precipitation coefficient was 0.77‰/100 mm, implying that, within physiological adaptation parameters, there would be a ~0.77‰ increase in $\delta^{13}C$ with a 100 mm increase in precipitation. The $\delta^{13}C$ values yielded by ancient common millets are slightly higher than those of modern common millet seeds, suggesting that these ancient plants grew in a much more humid environment than today's.

Common millet remains from archeological sites were divided into a total of 11 groups (Table 3). Mean $\delta^{13}C$ values for common millet remains were calculated for each group. Results showed that the minimum value was -10.55±0.16‰, and the maximum value -9.56±0.09‰, for common millet growing between 7.7 ka BP and 3.4 ka BP. After correcting for the change in the atmospheric CO_2 $\delta^{13}C$ (1.8‰), the range of mean $\delta^{13}C$ values for ancient millet *vis-à-vis* modern plants was between -12.35‰ and -11.36‰. By applying the regression model based on the $\delta^{13}C$ and precipitation values for modern common millet during its growing season, we were able to extract paleoprecipitation values for the growing seasons of ancient crops for certain time periods.

These paleoprecipitation values were reconstructed by applying the $\delta^{13}C_{re}$ values for the ancient millet to a regression equation (Eq. 2) which expresses the relation between the $\delta^{13}C$ of common millet and precipitation. The results showed that the precipitation for the growing seasons (P_{gs}) of ancient millet during the period 7.7-3.4 ka BP varied from 240 mm to 477 mm, with a mean of 354 mm (Table 3).

4 Discussion

4.1 The rationale behind using common millet $\delta^{13}C$ for precipitation reconstruction

Carbon isotope composition of fossilized plant remains is a useful proxy for the reconstruction of local paleoclimatic changes, especially when using $\delta^{13}C$ values from plants which experience a single mode of photosynthesis. Common millet grains have been widely and continuously preserved throughout the Holocene in northern China. Fossilized millet seeds were generally formed at low temperatures (~250℃) by baking (Yang *et al*., 2011a), and deposited in strata over long time periods with limited interaction with the buried environment. The observed $\delta^{13}C$ values of charred common millet formed at ~250℃ were 0.2‰ lower than those of the source samples,

Clim. Past Discuss., doi:10.5194/cp-2016-87, 2016
Manuscript under review for journal Clim. Past
Published: 29 August 2016

Climate of the Past Discussions
Open Access
EGU

and much less than the natural variation typically found in wood (Yang *et al*., 2011b). The $\delta^{13}C$ signatures conserved in carbonized common millet are thus more reflective of the true environment, without artificial correction.

The Carbon isotope composition of plants ($\delta^{13}C_p$) is affected by both physiological characteristics and environmental factors. The $\delta^{13}C$ of C_3 plants responds to environmental factors, such as atmospheric CO_2 pressure, O_2 partial pressure, temperature, light and precipitation, by dominating the ratio of the intercellular and ambient partial pressure of CO_2 (c_i/c_a) with the opening and closing of leaf stomata (Körner and Diemer, 1987; Körner and Larcher, 1988; Körner *et al*., 1989; Farquhar *et al*., 1989; Dawson *et al*., 2002). However, the $\delta^{13}C$ of C_4 plants depends not only on c_i/c_a but also on how much CO_2 and $H\bar{C}O_3^-$ in bundle sheath cells leaks into the mesophyll cells (called leakiness φ), which is determined by its physiological characteristics (Hubick *et al*., 1990). When φ is larger/smaller than 0.37, there is a positive/negative correlation between $\delta^{13}C_p$ and c_i/c_a (Ubierna *et al*., 2011). Under water stress, the φ of the common millet, belonging to the NADP-ME subgroup of C_4 plants, is likely larger than 0.37 (Schulze *et al*., 1996; Yang and Li, 2015). This may account for the relation between the $\delta^{13}C$ of common millet and precipitation being significantly positive (Yang and Li, 2015).

Limited precipitation and soil humidity are the most important environmental factors affecting the growth of plants in arid and semi-arid areas (IPCC, 2007). For C_4 species in the arid regions of northwestern China, $\delta^{13}C_p$ tends to decrease with decreasing soil water availability (Wang *et al*., 2005b). For common millet, although altitude, precipitation and water availability have a significant correlation with $\delta^{13}C$ according to correlation analysis, precipitation was the principal control of $\delta^{13}C$, based on functional mechanism analysis (Yang and Li, 2015). The plants' physiological characteristics and morphological adaptability showed that the stomatal, and some non-stamatal, factors of common millet are sensitive to water status, causing the $\delta^{13}C$ of the organic material to change with precipitation. This rationale establishes an important theoretical foundation whereby the $\delta^{13}C$ of common millet can serve as an effective indicator of paleoprecipitation.

4.2 Comparison between the mid-Holocene and modern precipitation

Ancient equivalent-seed $\delta^{13}C$ values, ranging from -12.35‰ to -11.36‰, are ~ 1–2‰ higher than those for modern millet seeds in the area. However, these analyses reveal a small but significant shift to lower $\delta^{13}C$ values in modern seeds. Based on the positive relation between the $\delta^{13}C$ of modern common millet and precipitation in the CLP, the observed increases in the $\delta^{13}C$ values of ancient millet seeds could have been caused by increased precipitation. Calculations using the regression equation provide conservative estimates of the magnitude of this $\delta^{13}C$ shift in precipitation.

The $\delta^{13}C$ values of common millet seeds reflect the ^{13}C of photosynthetic materials during not only their formative and mature stages, but also their vegetative stage. The growing season of modern common millet in the Guanzhong Basin lasts from June to September. The seed kernel's formative and mature stages occur soon

Clim. Past Discuss., doi:10.5194/cp-2016-87, 2016
Manuscript under review for journal Clim. Past
Published: 29 August 2016

Climate of the Past Discussions
Open Access
EGU

after pollination of the blossom. With an increase in kernel size, photosynthetic material as well as pre-accumulated organic material is transferred to kernels from stems, leaves and spikes (Chai, 1999). Therefore, millet $\delta^{13}C$ reflects the environmental conditions extant during the growing season from mid-June to the end of September, or 110 days in total.

Precipitation data from the Guanzhong Basin for the period 1951-2011 were analyzed. The results showed that the precipitation for mid-June to September was between 110-526 mm, with a mean of 305 mm (Figure 4). The 95% confidence interval for this mean is between 279-332 mm, ruling out the extreme values of abnormal years. Paleoprecipitation reconstructed from the regression function shows that growing season precipitation for millet from 7.7-3.4 ka BP was between 240 and 477 mm, with a mean of 354 mm. Summer paleoprecipitation values show that the climate was much more humid than it is today, with mean precipitation ~50 mm, or 17%, higher. A peak mean summer precipitation of 442 mm was reached at ~5.7 ka BP; even the lowest value of 313 mm ~6.5 ka BP was higher than today's mean value. Summer precipitation during the Mid Holocene (7.7-3.4 ka BP) in the Guanzhong Basin exhibited a systemic increase.

The reconstructed summer precipitation also fluctuates significantly. Accordingly, the 7.7-3.4 ka BP period can be divided into four distinct stages (Figure 4). During the 7.7-6.4 ka period, summer precipitation was 332 mm, which is 9%, or 27 mm, higher than today. For 6.4-5.5 ka BP, summer precipitation was 414 mm, *i.e.* 109 mm, or 36%, higher than today. During 5.5-4.4 ka BP, summer precipitation was 338 mm, higher than today's value by 33 mm, or 11%. During the period 4.4-3.4 ka BP, summer precipitation was 361 mm, *i.e.* 18%, or 56 mm, higher than today.

On the basis of the above analysis, the period 6.4-5.5 ka BP, having the most abundant precipitation and being the most markedly humid period, probably marks the Holocene Climate Optimum in the Guanzhong Basin; this was also when the Yangshao Culture flourished, with archeological finds indicating that there were as many villages in the area as there are today. It is worth noting that the relatively high precipitation during 4.4-3.4 ka BP was mainly caused by an anomalous high value of 397±11 mm at ~4.1 ka BP, when precipitation was 92 mm, or 30% higher, than at present. This may indicate a rapidly-developing climatic event, correspondent with other global records.

4.3 Validating the reliability of quantitative precipitation reconstructions

The instrumental data for the last 60 years (1961-2011) indicate that precipitation in the Guanzhong Basin occurs mainly in the summer (Figure 5). The current inland flow of warm/humid air dominated by the EASM during the summer (June through September) delivers ~58% of the total annual precipitation. The area is a typical monsoon precipitation area, and summer precipitation here is therefore sensitive to variations in the EASM.

Previous studies of various climatic proxies including stalagmite $\delta^{18}O$, lacustrine sediments and loess-paleosols all indicate that the CLP had plenty of rain in the Holocene and was much more humid during the Mid Holocene (Shen *et al*., 2005;

Clim. Past Discuss., doi:10.5194/cp-2016-87, 2016
Manuscript under review for journal Clim. Past
Published: 29 August 2016

Wang *et al*., 2005a; Wang *et al*., 2008; Wang *et al*., 2014; Chen *et al*., 2015). The frequency of paleosol development increased during ~8.6-3.2 ka in the CLP (Wang *et al*., 2014). The eolian-sand activities in the sandlands located to the north of the CLP decreased from ~8.6-3.2 ka BP (Wang *et al*., 2014; Yang *et al*., 2012), whilst the vegetation coverage of the desert/loess transitional zone increased in this interval (Yang *et al*., 2015). These various proxy records infer that the EASM was stronger during the Mid Holocene, but the amplitude of any variations in the EASM remains difficult to assess. Fortunately, summer precipitation in northern China provides an effective approach to determining EASM intensity (Liu *et al*., 2015).

Our quantitative reconstructions of summer precipitation based on millet $\delta^{13}C$ indicate that EASM intensity peaked during 6.4-5.5 ka BP. The strongest summer monsoon brought the wettest climate, with 36% higher precipitation than today's. More evidence supporting our contention comes from the tree pollen records from lake sediments around the CLP, which respond more directly to changes in the EASM than the other records because trees on the margins of monsoonal regions are sensitive to variations in monsoonal precipitation. Pollen records from Qinghai Lake, located to the west of the Guanzhong Basin and on the modern monsoon margins, indicate a wet interval during 7.4-4.5 ka BP, culminating in a peak at 6.5 ka BP (Figure 6a) (Shen *et al*., 2005). Although the increase in precipitation cannot be assessed, the general trend is comparable with our $\delta^{13}C$-based precipitation reconstruction results. The percentage of broadleaf trees from pollen record in the Gonghai Lake (on the northeastern margins of the CLP; Figure 6b), indicate that the peak monsoonal period occurred during ~7.8-5.3 ka BP, with an average annual precipitation of 574 mm (Figure 6c), ~30% higher than the modern value (Chen *et al*., 2015). The increase in precipitation is highly consistent with our reconstruction results. More evidence from PMIP2 (the second phase of the Paleoclimate Modeling Intercomparison Project) coupled with Mid Holocene simulations showed that the summer precipitation associated with the EASM increased throughout most of China ~6 ka BP. The increase in precipitation in the Guanzhong Basin was lower than 255.5 mm/yr at that time, as inferred from the greatest increases in precipitation seen in the region, *i.e.* the southern margins of the Tibetan Plateau, and southeastern coastal area of China, which experienced precipitation increases of >1.5 mm/day and 0.7 mm/day (or 547.5 mm/yr and 255.5 mm/yr), respectively (Zhang and Liu, 2009). These multiple lines of evidence corroborate our reconstructions, not only *vis-à-vis* changes in precipitation during the Holocene, but also their quantitative accuracy.

5 Conclusions

Summer precipitation from 7.7 to 3.4 ka BP reconstructed using the $\delta^{13}C$ values of common millet was 240-477 mm, with a mean of 354 mm, ~50 mm, or 17%, higher than at present. Maximum mean summer precipitation peaked at 414 mm, ~109 mm (or 36%) higher than today; this occurred during the period 6.4-5.5 ka BP, indicating that the EASM peaked at this time.

Although the $\delta^{13}C$-based precipitation record in this study has a low-resolution, the work provides a convincing method and proxy for establishing the

Clim. Past Discuss., doi:10.5194/cp-2016-87, 2016
Manuscript under review for journal Clim. Past
Published: 29 August 2016

paleoprecipitation record. Carbonized common millet remains from the Neolithic Age onward can provide a reliable dating framework and aid the reconstruction of continuous paleoprecipitation sequences. This, in turn, can allow regional comparisons, providing a scientific foundation for promoting further research into the quantitative reconstruction of regional paleoclimates, and helping to understand the detailed processes and precise mechanisms of the EASM, as well as the relation between early human activity and environmental change.

Authorial contributions

X. Q. L.: overall coordination of writing, sampling, ^{14}C dating and paleoprecipitation reconstruction; Q. Y.: writing, sampling, data processing and paleoprecipitation reconstruction; X. Y. Z. and K. L. Z.: sampling and data processing; N. S.: sampling and ^{14}C dating. All authors reviewed the manuscript.

Acknowledgements

This study was supported by the National Basic Research Program of China (Grant No. 2015CB953804, 2015CB953803), the National Natural Science Foundation of China (Grant Nos. 41301042, 41372175) and the National Science Fund for Talent Training in Basic Science (Grant No. J1210008). We thank Prof. John Dodson for AMS^{14}C dating support, and Dr. Ying Xi for assistance with collecting the original meteorological data.

References

An, Z. M.: Prehistoric agriculture in China, Acta. Archaeol. Sin., 4, 369–381, in Chinese, 1988.

An, Z. S., Porter, S. C., Kutzbach, J. E, Wu, X. H., Wang, S. M., Liu, X. D., Li, X. Q., and Zhou, W. J.: Asynchronous Holocene optimum of the East Asian monsoon, Quatern. Sci. Rev., 19, 743-762, 2000.

Araus, J. L., and Buxo, R. Changes in carbon isotope discrimination in grain cereals from the north-western Mediterranean Basin during the past seven millennia, Aust. J. Plant. Physiol., 20, 117-128, 1993.

Bond, G., Showers, W., Cheseby, M., Lotti, R., Almasi, P., deMenocal, P., Priore. P., Cullen, H., Hajdas, I., and Bonani, G.: A pervasive millennial-scale cycle in North Atlantic Holocene and glacial climates, Science, 278(5341), 1257-1266, 1997.

Caley, T., Roche, D. M. and Renssen, H.: Orbital Asian summer monsoon dynamics revealed using an isotope-enabled global climate model, Nat. Commun., 5, 5371, 2014.

Chai, Y.: Broomcorn millet, Chinese Agriculture Press, Beijing, China, 47-70, 1999.

Chen, F. H., Xu, Q. H., Chen, J.H., Birks, H. J. B., Liu, J. B., Zhang, S. R., Jin, L., An, C. B., Telford, R. J., Cao, X. Y., Wang Z. L., Zhang, X. J., Selvaraj, K., Lu, H. Y., Li, Y.C., Zheng, Z., Wang, H. P, Zhou, A.F., Dong, G.H., Zhang, J. W., Huang, X. Z., Bloemendal, J., and Rao, Z.G.: East Asian summer monsoon precipitation variability since the last deglaciation, Sci. Rep., 5, 11186, 2015.

Cheng, H., Edwards, R.L., Broecker, W. S., Denton, G.H., Kong, X., Wang. Y., Zhang, R., Wang, X.: Ice Age Terminations, Science, 326, 248-252, 2009.

Clim. Past Discuss., doi:10.5194/cp-2016-87, 2016
Manuscript under review for journal Clim. Past
Published: 29 August 2016

Climate of the Past Discussions
Open Access
EGU

437 Cuntz, M.: Carbon cycle: A dent in carbon's gold standard, Nature, 477, 547–548, 2011.
438 Dawson, T.E., Mambelli, S., Plamboeck, A. H., Templer, P. H., and Tu, K. P.: Stable Isotopes in
439 Plant Ecology, Annu. Rev. Ecol. Syst., 33, 507–559, 2002.
440 DeMenocal, P. B.: Cultural responses to climate change during the late Holocene, Science, 292,
441 667-673, 2001.
442 Dore, M. H. I.: Climate change and changes in global precipitation patterns: What do we know?,
443 Environ. Int., 31, 1167-1181, 2005.
444 Falster, D. S., Warton, D. I., and Wright, I. J.: User's guide to SMATR: Standardised Major Axis
445 Tests & Routines Version 2.0, Copyright 2006, 2006,
446 http://www.bio.mq.edu.au/ecology/SMATR/
447 Farquhar, G. D., Ehleringer, J. R., and Hubick, K. T.: Carbon isotope discrimination and
448 photosynthesis, Annu. Rev. Plant Physiol. Mol. Biol., 40, 503-537, 1989.
449 Genty, D., Blamart, D., Ouahdi, R., Gilmour, M., Baker, A., Jouzel, J., Van-Exter, S.: Precise
450 dating of Dansgaard–Oeschger climate oscillations in western Europe from stalagmite data,
451 Nature, 421, 833-837, 2003.
452 Guo, Z. T., Liu, T., Guiot, J., Wu, N., L, H., Han, J., Liu, J., Gu, Z.: High frequency pulses of East
453 Asian monsoon climate in the last two glaciations: link with the North Atlantic, Clim. Dynam,
454 12, 701-709, 1996.
455 Hatté, C., and Guiot, J.: Palaeoprecipitation reconstruction by inverse modelling using the isotopic
456 signal of loess organic matter: application to the Nußloch loess sequence (Rhine Valley,
457 Germany), Clim Dynam, 25, 315-327, 2005.
458 Hubick, K.T., Hammer, G. L., Farquhar, G. D., Wade, L. J., von Caemmerer, S., and Henderson, S.
459 A.: Carbon isotope discrimination varies genetically in C4 species, Plant. Physiol., 92, 534–537,
460 1990.
461 IPCC: Climate Change 2007: The Physical Science Basis, Solomon, S. et al. Cambridge, 2007
462 Keeling, C. D., and Whorf, T. P. in: Atmospheric CO_2 – modern record, Mauna Loa, edited by:
463 Boden, T A, Sepanski, R. J. and Stoss, F. W.: Trends 91: A Compendium of Data on Global
464 Change, ORNL/CDIAC-46, Carbon Dioxide Information Analysis Center, Oak Ridge National
465 Laboratory, Oak Ridge, Tennessee, USA, 12-15, 1992.
466 Kleiven, H. K. F., Kissel, C., Laj, C., Ninnemann, U. S., Richter, T. O., and Cortijo, E.: Reduced
467 North Atlantic deep water coeval with the glacial Lake Agassiz freshwater outburst, Science,
468 319(5859), 60-64, 2008.
469 Körner, C. H., and Diemer, M.: *In situ* photosynthetic responses to light, temperature and carbon
470 dioxide in herbaceous plants from low and high altitude, Funct. Ecol., 1(3), 179-194, 1987.
471 Körner, C. H., and Larcher, W. Plant life in cold climates, Symp Soc Exper Biol., 42, 25–57,
472 1988.
473 Körner, C. H., Newmayer, M., Palaez Menendez-Reidl, S., and Smeets-Scheel, A.: Functional
474 morphology of mountain plants, Flora, 182, 353-383, 1989.
475 LeGrande, A., and Schmidt, G.: Sources of Holocene variability of oxygen isotopes in
476 paleoclimate archives, Clim. Past, 5, 441-455, 2009.
477 Lei, X. S.: Pre-Zhou culture exploration, Science Press, Beijing, China, in Chinese, 2010.
478 Leuenberger, M., Siegenthaler, U., and Langway, C. C.: Carbon isotope composition of
479 atmospheric CO_2 during the last ice age from an Antarctic ice core, Nature, 357, 488-490, 1992.
480 Liu, C. J., Jin, G. Y., and Kong, Z. C.: Archaeobotany — Research on Seeds and Fruits, Science

Clim. Past Discuss., doi:10.5194/cp-2016-87, 2016
Manuscript under review for journal Clim. Past
Published: 29 August 2016

Climate of the Past Discussions
Open Access
EGU

Press, Beijing, China, pp. 160-171, 2008.

Liu, J.B., Chen, J.H., Zhang, X. J., Li, Y., Rao, Z. G., and Chen, F. H.: Holocene East Asian summer monsoon records in northern China and their inconsistency with Chinese stalagmite $\delta^{18}O$ records, Earth-Sci. Rev., 148, 194-208, 2015.

Lu, H. Y., Han, J. M., Wu, N. Q., and Guo Z. T.: The analysis of modern soil magnetic susceptibility and its paleoclimate significance, Sci. China, Ser. B, 24(12), 1290-1297, in Chinese, 1994.

Lu, H. Y., Wu, N. Q., Liu, T. S., Han, J. M., and Qin X. G.: Seasonal climatic variation recorded by phytolith assemblages from the Baoji loess sequence in central China over the last 150 000, Sci. China, Ser. D, 39(6), 629-639, 1996.

Lu, H. Y., Zhang, J. P., Liu, K.-B., Wu, N. Q., Li, Y. M., Zhou, K. S., Ye, M. L., Zhang, T. Y., Zhang, H. J., Yang, X. Y., Shen, L. C., Xu, D. K., Li, Q., and Piperno, D. R.: Earliest domestication of common millet (*Panicum miliaceum*) in East Asia extended to 10,000 years ago, P. Natl. Acad. Sci. U.S.A., 18, 7367-7372, 2009.

Maher, B. A., and Thompson, R.: Oxyen isotopes from Chinese caves: records not of monsoon rainfall but of circulation regime, J. Quat. Sci., 27, 615-624, 2012.

Marcott, S. A., Shakun, J. D., Clark, P. U., and Mix, A.C.: A reconstruction of regional and global temperature for the past 11,300 years, Science, 339(6124), 1198-1201, 2013.

Marino, B. D., McElroy, M. B., Salawitch, R. J., and Spaulding, W. G.: Glacial-to-interglacial variations in the carbon isotopic composition of atmospheric CO_2, Nature, 357, 461-466, 1992.

Mayewski, P. A., Rohling, E. E., Stager, J. C., Karlén, W., Maasch, K. A., Meeker, L. D., Meyerson, E. A., Gasse, F., van Kreveld, S., Holmgren, K, Lee-Thorp, J., Rosqvist, G., Rack, F., Staubwasser, M., Schneider, R. R., and Steig, E. J.: Holocene climate variability, Quatern. Res., 62(3), 243-255, 2004.

Porter, S. C., and An, Z. S.: Correlation between climate events in the North Atlantic and China during the last glaciation, Nature, 375, 305-308, 1995.

Prentice, I. C., and Webb III, T.: BIOME 6000: reconstructing global mid□Holocene vegetation patterns from palaeoecological records, J. Biogeogr. 25, 997-1005, 1998.

Reimer, P. J., Bard, E., Bayliss, A., Beck, J. W., Blackwell, P. G., Ramsey, C. B., Buck, C. E., Hai C., Edwards, R. L., Friedrich, M., Grootes, P. M., Guilderson, T. P., Haflidason, H., Hajdas, I., Hatté, C., Heaton, T. J., Hoffmann, D. L., Hogg, A. G., Hughen, K. A., and Kaiser, K. F.: IntCal13 and Marine13 radiocarbon age calibration curves 0-50,000 years cal BP, Radiocarbon 55(4), 1869-1887, 2013.

Ren, S. N., and Wu, Y. L.: The Neolithic Volume of Chinese Archaeology, Chinese Social Science Press, Beijing, China, in Chinese, 2010.

Schulze, E.-D., Ellis, R., Schulze, W., Trimborn, P., and Ziegler, H.: Diversity, metabolic types and $\delta^{13}C$ carbon isotope ratios in the grass flora of Namibia in relation to growth form, precipitation and habitat conditions, Oecologia, 106, 352-369, 1996.

Shen, J., Liu, X. Q., Wang, S. M., and Ryo, M.: Palaeoclimatic changes in the Qinghai Lake area during the last 18,000 years, Quat. Int., 136, 131-140, 2005.

State Cultural Relics Bureau (ed): Atlas of Chinese Cultural Relics: Shannxi Municipality, Xi'an Map Press, Xi'an, China, in Chinese, 1998.

Sun, J. M., Diao, G. Y., Wen, Q. Z., and Zhou, H. Y.: A preliminary study on quantitative estimate of Palaeoclimate by using geochemical transfer function in the Loess Plateau,

Clim. Past Discuss., doi:10.5194/cp-2016-87, 2016
Manuscript under review for journal Clim. Past
Published: 29 August 2016

525 Geochim, 28(3), 265-272, in Chinese, 1999.
526 Sun, N., Li, X. Q., Dodson, J., Zhou, X. Y., Zhao, K. L., Yang, Q.: Plant diversity of the Tianshui
527 Basin in the western Loess Plateau during the mid-Holocene – charcoal records from
528 archaeological sites, Quatern. Int, 308-309, 27-35, 2012.
529 Sun, N., and Li, X. Q.: The quantitative reconstruction of the palaeoclimate between 5200 and
530 4300 cal yr BP in the Tianshui Basin, NW China, Clim. Past, 8, 625-636, 2012.
531 Tan, M.: Circulation effect: response of precipitation $\delta^{18}O$ to the ENSO cycle in monsoon
532 regions of China, Clim. Dyn., 42, 1067-1077, 2012.
533 Tsuyuzaki, S.: Rapid seed extraction from soils by a flotation method, Weed Res., 34, 433-436,
534 1994.
535 Ubierna, N., Sun, W., and Cousins, A. B.: The efficiency of C_4 photosynthesis under low light
536 conditions: assumptions and calculations with CO_2 isotope discrimination, J. Exp. Bot., 1–16,
537 2011.
538 Wang, H., Chen, J., Zhang, X., and Chen, F.: Palaeosol development in the Chinese Loess Plateau
539 as an indicator of the strength of the East Asian summer monsoon: Evidence for a mid-
540 Holocene maximum, Quaternary International, 334, 155-164, 2014.
541 Wang, Y. J., Cheng H., Edwards, R. L., He Y. Q., Kong, X. G., An, Z. S., Wu, J. Y., Kelly, M. J.,
542 Dykoski, C. A., and Li, X. D.: The Holocene Asian monsoon: links to solar changes and North
543 Atlantic climate, Science, 308, 854-857, 2005a.
544 Wang, G.A., Han, J. M., Zhou, L. P., Xiong, X. G, and Wu, Z. H.: Carbon isotope ratios of plants
545 and occurrences of C_4 species under different soil moisture regimes in arid region of Northwest
546 China, Physiol.Plant., 125, 74–81, 2005b.
547 Wang, Y. J., Cheng, H., Edwards, R. L., Kong, X. G., Shao, X. H., Chen, S. T., Wu, J. Y., Jiang,
548 X. Y., Wang, X. F., and An, Z. S.: Millennial- and orbital-scale changes in the East Asian
549 monsoon over the past 224,000 years, Nature, 451, 1090-1093, 2008.
550 Warton, D. I., Wright I. J., Falster, D. S., and Westoby, M.: Bivariate Line-fitting methods for
551 allometry, Biol. Rev., 81, 259-291, 2006.
552 Yang, Q., Li, X. Q., Zhou, X.Y., Zhao, K. L., Ji, M., and Sun, N.: Investigation of the
553 ultrastructural characteristics of foxtail and broomcorn millet during carbonization and its
554 application in archaeobotany, Chinese. Sci. Bull, 56(14), 1495-1502, 2011a.
555 Yang, Q., Li, X. Q., Liu, W. G., Zhou, X.Y., Zhao, K. L., and Sun, N.: Carbon isotope
556 fractionation during low temperature carbonization of foxtail and common millets, Org.
557 Geochem., 42, 713-719, 2011b.
558 Yang, L. H., Wang, T., Zhou, J., Lai, Z. P., and Long, H.: OSL chronology and possible forcing
559 mechanisms of dune evolution in the Horqin dunefield in northern China since the Last Glacial
560 Maximum, Quatern. Res., 78, 185-196, 2012.
561 Yang, Q., and Li, X. Q.: Investigation of the controlled factors influencing carbon isotope
562 composition of foxtail and common millet on the Chinese Loess Plateau, Sci. China Ser D,
563 58(12), 2296-2308, 2015.
564 Yang, Q., Li, X.Q., and Zhou, X.Y.: Vegetation Succession Responding to Climate Changes since
565 LGM in Desert-Loess Transition Zone, North China, Acta. Antherop. Sin., DOI:
566 10.16359/j.cnki.cn11-1963/q.2015.0000, in Chinese with English abstract , 2015.
567 Zhang, R and Liu, X. D.: An analogy analysis of summer precipitation change patterns between
568 mid-Holocene and future climatic warming scenarios over East Asia, Sci. Geogr. Sin., 29(5),

Clim. Past Discuss., doi:10.5194/cp-2016-87, 2016
Manuscript under review for journal Clim. Past
Published: 29 August 2016

679-683, in Chinese with English abstract, 2009.

Zhao, J. B.: Soil developed in the Holocene Megathermal and climatic migration in the Guanzhong area, Sci. Geogr. Sinia, 23(5), 554-559, 2003. (in Chinese with English abstract).

Zhao, Z. J., and Xu L. G.: The tentative flotation result and preliminary analysis in Zhouyuan ruins (Wangjiazui site), Cult. Rel., (10), in Chinese, 89-96, 2004.

Clim. Past Discuss., doi:10.5194/cp-2016-87, 2016
Manuscript under review for journal Clim. Past
Published: 29 August 2016

Climate of the Past Discussions
Open Access
EGU

Tables

Table 1 Sampling sites and numbers of remnant common millet samples

Sites	Cultural types	Source	No.
BJC	Early Laoguantai Culture	12	
HDP	Banpo type, Yangshao Culture	Cultural layers	9
MN	Miaodigou type, Yangshao Culture	Cultural layers	11
BN	Longshan Culture	Cultural layers	15
NS	Erlitou Culture, Shang Dynasty	Cultural layers	20

Table 2 AMS^{14}C dating data

Sample code	Depth (cm)	Sample type	AMS ^{14}C age (cal yr BP)	Calibrated age range (cal yr BP, 2σ)	Lab code
BJC-1	180-190	Common millet	6,705±40	7,580±76	OZM447
BJC-2	50-60	Charcoal	6,675±40	7,543±68	OZM446
HDP-1	235-250	Common millet	5,720±50	6,523±115	OZM473
HDP-2	160-180	Rice seed	5,015±45	5,775±120	OZM472
HDP-3	80-100	Rice seed	5,120±35	5,790±40	OZM471
HDP-4	40-60	Foxtail millet	5,185±40	5,948±59	OZM470
MN-1	140-160	Foxtail millet	4,550±35	5,121±70	OZM452
BN-1	280-300	Foxtail millet	5,450±70	6,286±113	OZM481
BN-2	220-240	Foxtail millet	3,820±45	4,191±109	OZM480
BN-3	180-200	Rice seed	3,770±35	4,158±85	OZM479
BN-4	120-140	Foxtail millet	4,540±50	5,181±141	OZM478
BN-5	40-60	Common millet	4,110±40	4,625±104	OZM477
NS-1	230-240	Wheat seed	3,300±30	3,521±70	OZM460
NS-2	200-210	Wheat seed	3,280±35	3,514±73	OZM459
NS-3	140-150	Wheat seed	3,300±30	3,521±70	OZM458

Table 3 Information for grouped common millet remains, by section

Section	Cultural age	Depth （cm）	N	^{14}C Age (cal yr BP)	Mean $\delta^{13}C$(‰)	$\delta^{13}C_{re}$ (‰)	P_S (mm)
BJC	Laoguantai Culture	50-190	12	7,475-7,656	-10.36±0.23	-12.16	337±30
HDP	Banpo type, Yangshao Culture	200-250	3	6,407-6,638	-10.55±0.29	-12.35	313±37
	Banpo type, Yangshao Culture	120-200	2	5,654-5,895	-9.56±0.12	-11.36	442±16
	Banpo type, Yangshao Culture	0-120	3	5,749-6,008	-9.87±0.09	-11.67	401±12
MN	Miaodigou type, Yangshao Culture	0-260	11	5,052-5,190	-10.37±0.36	-12.17	336±47
BN	Yangshao Culture	260-300	2	6,171-6,399	-9.84	-11.64	405
	Longshan Culture	200-260	3	4,137-4,359	-10.23±0.04	-12.03	354±5
	Longshan Culture	140-200	3	4,072-4,243	-9.9±0.09	-11.70	397±11
	Longshan Culture	60-140	4	5,039-5,322	-10.28±0.21	-12.08	348±27
	Longshan Culture	40-60	2	4,520-4,729	-10.42±0.07	-12.22	330±9
NS	Erlitou Culture, Shang Dynasty	50-300	20	3,444-3,592	-10.23±0.36	-12.02	356±54

Clim. Past Discuss., doi:10.5194/cp-2016-87, 2016
Manuscript under review for journal Clim. Past
Published: 29 August 2016

Climate of the Past Discussions
Open Access
EGU

585 # Figures

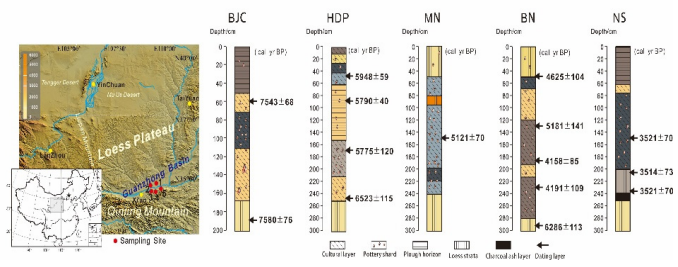

586

587 **Figure 1.** Location of sampling sites and description of all sampling sections. Red solid circles
588 indicate sampling sites. 1, Baijiacun site (BJC) (34°33′7.53″N, 109°24′38.6″E); 2, Huiduipo site
589 (HDP) (34°34′4.1″N, 109°01′41.8″E); 3, Manan site (MN) (34°28′23.7″N, 109°05′17.5″E); 4,
590 Beiniu site (BN) (34°28′14.5″N, 109°19′2.6″E); 5, Nansha site (NS)(34°29′30.1″N,
591 109°42′47.9″E). The map was created using Global Mapper 14.0 software
592 (http://www.skycn.com/soft/appid/11312.html) and NASA STRM data with a resolution of 90 m;
593 profiles were then drawn and combined with the map using CorelDRAW 12 software
594 (http://www.xp85.com/html/CorelDRAW12.html).
595
596

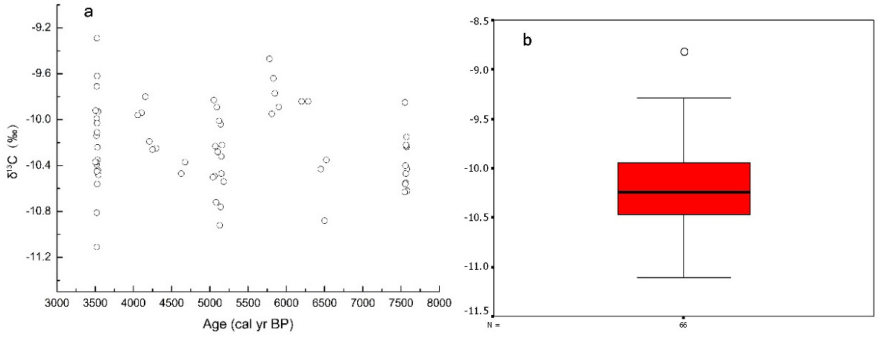

597

598 **Figure 2.** $\delta^{13}C$ of common millet from archeological sites, Guanzhong Basin
599
600

Clim. Past Discuss., doi:10.5194/cp-2016-87, 2016
Manuscript under review for journal Clim. Past
Published: 29 August 2016

Climate of the Past Discussions
Open Access
EGU

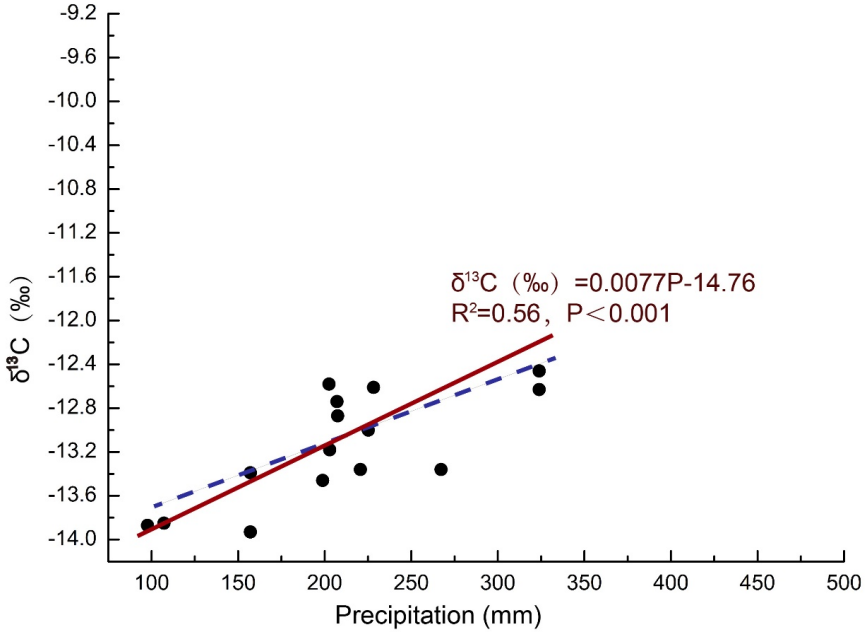

601

602 **Figure 3.** The regression model of the $\delta^{13}C$ of modern common millet and summer precipitation.

603 Dark red line denotes the line of best fit established using SMA; the blue dotted line denotes the

604 line of best fit established using OLS.

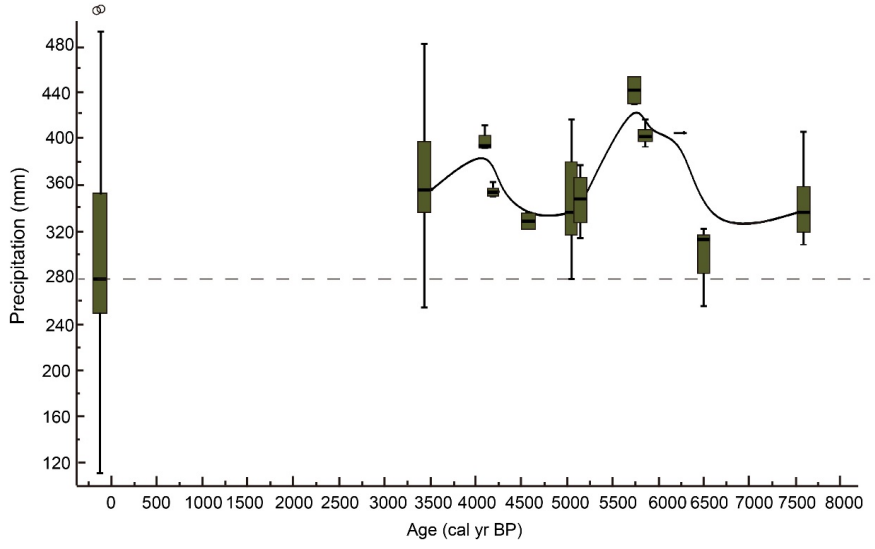

605

606 **Figure 4.** Precipitation for mid-June to September for a modern period (original data for 1951–

607 2011, from the China Meteorological Administration) and 7.7-3.4 ka BP, Guanzhong Basin

608

Clim. Past Discuss., doi:10.5194/cp-2016-87, 2016
Manuscript under review for journal Clim. Past
Published: 29 August 2016

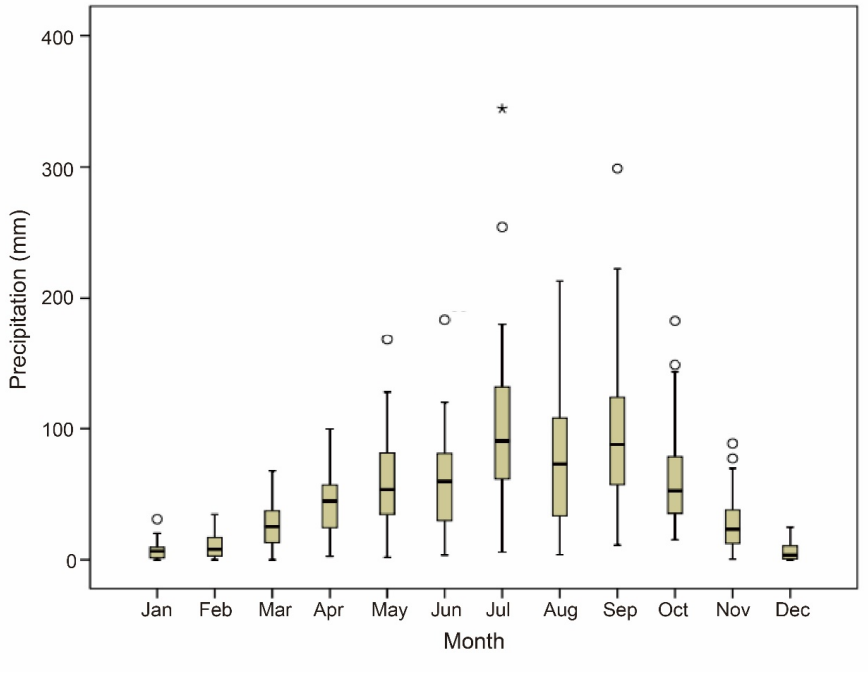

609

610 **Figure 5.** Instrumental precipitation data for 1951-2011 from Xi'an Station, Sha'anxi, China
611 (original data, Data Sharing Platform, China Meteorological Administration). The empty circle (o)
612 indicates an abnormal value; the asterisk (*) indicates an extremely abnormal value.

613

Clim. Past Discuss., doi:10.5194/cp-2016-87, 2016
Manuscript under review for journal Clim. Past
Published: 29 August 2016

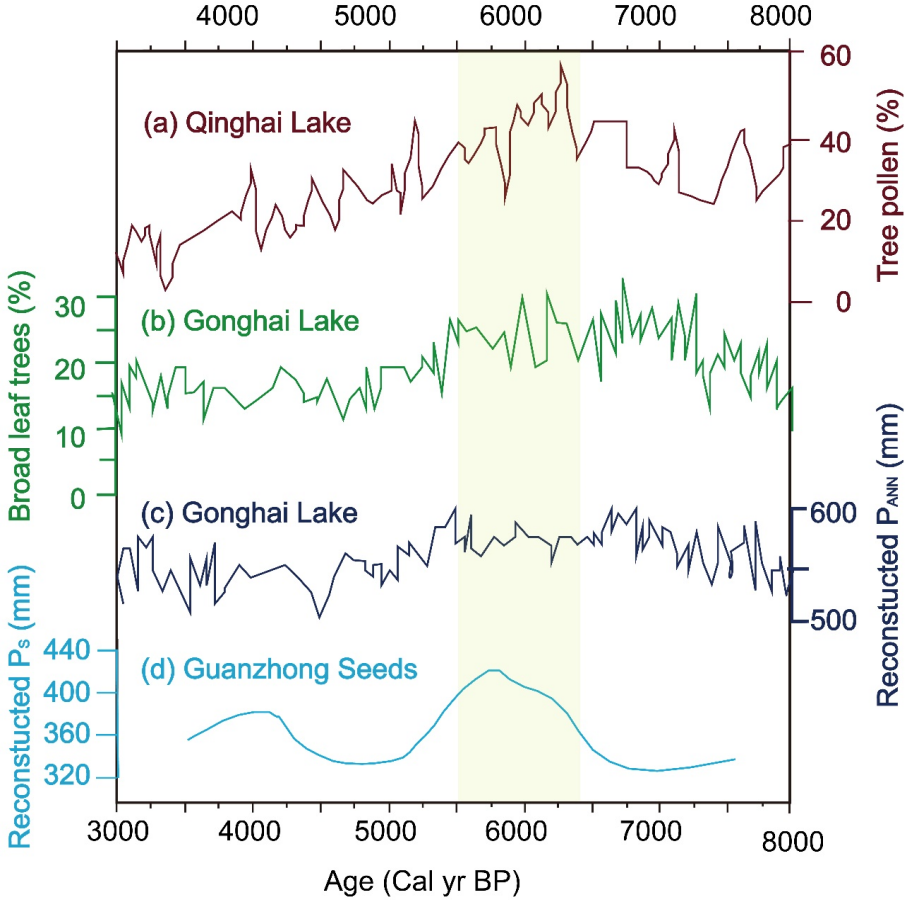

Figure 6. Comparison of reconstructed summer precipitation for 7.7-3.4 ka BP, Guanzhong Basin, with the pollen records of lakes sediments from around the CLP. (**a**) Tree pollen percentages from Qinghai Lake (Shen *et al*., 2005). (**b**) Broadleaf tree pollen percentages from Gonghai Lake (Chen *et al*., 2015). (**c**) Reconstructed annual precipitation from the pollen records of Gonghai Lake (Chen *et al*., 2015). (**d**) Reconstructed summer precipitation from the $\delta^{13}C$ values of common millet, Guanzhong Basin.